DMD Fast Forward. Published on September 11, 2008 as doi:10.1124/dmd.108.022970

DMD#22970

CONFIRMATION THAT CYTOCHROME P450 2C8 (CYP2C8) PLAYS A MINOR ROLE IN (*S*)-(+)- AND (*R*)-(-)-IBUPROFEN HYDROXYLATION IN VITRO

Shu-Ying Chang, Wenying Li, Sarah C. Traeger, Bei Wang*, Donghui Cui, Hongjian Zhang, Bo Wen, and A. David Rodrigues

Bristol-Myers Squibb, Princeton, New Jersey, USA (SYC, WL, SCT, BW* and ADR), Merck Research Laboratories, West Point, Pennsylvania, USA (DC), Roche, Palo Alto, California, USA (BW), and PharmaResources Co., Shanghai, China (HZ)

DMD#22970

Running Title: Ibuprofen enantiomer metabolism by CYP2C8 and CYP2C9

Corresponding Author:

Ms. Shu-Ying Chang, Bristol-Myers Squibb, 311 Pennington-Rocky Hill Rd., NJ 08534

TEL: (609) 818-7649, e-mail: shu.chang@bms.com

Number of text pages	21
Number of Tables:	2
Number of Figures:	5
Number of references:	40
Number of words in *Abstract*:	265
Number of words in the *Introduction*:	497
Number of words in the *Discussion*:	1459

Abbreviations. Cytochromes P450, P450; HLM, human liver microsomes; LC-MS/MS, liquid chromatography-tandem mass spectrometry; HPLC, high-performance liquid chromatography; rCYP2C8, recombinant cytochrome P450 2C8; rCYP2C9, recombinant cytochrome P450 2C9; AUC, area under the plasma concentration versus time curve; HPLC, high-performance liquid chromatography; V_{max}, maximal initial rate of reaction; K_m, Michaelis constant; CL_{int}, intrinsic clearance (V_{max}/K_m); IBU, ibuprofen; 2-OH, 2-hydroxy-ibuprofen; 3-OH, 3-hydroxy-ibuprofen; Mabs, monoclonal antibodies; NMR, nuclear magnetic resonance; ADME, absorption-distribution-metabolism-excretion; (*S*)-(+)-IBU, (*S*)-(+)-ibuprofen; (*R*)-(-)-IBU, (*R*)-(-)-ibuprofen; 3-carboxy-IBU, 3-carboxy-ibuprofen; THF, tetrahydrofuran; OATP, organic anion transporting peptide; PK, pharmacokinetics.

Abstract

Various groups have sought to determine the impact of *CYP2C8* genotype (and CYP2C8 inhibition) on the pharmacokinetics (PK) of ibuprofen (IBU) enantiomers. However, the contribution of cytochrome P450 2C8 (CYP2C8) in human liver microsomes (HLM) has not been reported. Therefore, in vitro cytochrome P450 (P450) reaction phenotyping was conducted with selective inhibitors of cytochrome P450 2C9 (CYP2C9) and CYP2C8. In the presence of HLM, sulfaphenazole (CYP2C9 inhibitor) and anti-CYP2C9 monoclonal antibodies (Mabs) inhibited (73 to 100%) the 2- and 3-hydroxylation of both IBU enantiomers (1 and 20 μM). At a higher IBU concentration (500 μM), the same inhibitors were less able to inhibit the 2-hydroxylation of (*S*)-(+)-IBU (32 to 52%) and (*R*)-(-)-IBU (30 to 64%), whereas the 3-hydroxylation of (*S*)-(+)-IBU and (*R*)-(-)-IBU was inhibited 66 to 83% and 70 to 89%, respectively. In contrast, less inhibition was observed with montelukast (CYP2C8 inhibitor, ≤ 35%) and anti-CYP2C8 Mabs (≤ 24%) at all concentrations of IBU. When (*S*)-(+)-IBU and (*R*)-(-)-IBU (1 μM) were incubated with a panel of recombinant human P450s, only CYP2C9 formed appreciable amounts of the hydroxy metabolites. At a higher IBU enantiomer concentration (500 μM), additional P450s catalyzed 2-hydroxylation (CYP3A4, CYP2C8, CYP2C19, CYP2D6, CYP2E1 and CYP2B6) and 3-hydroxylation (CYP2C19). When P450 reaction phenotype and additional clearance pathways are considered (e.g., direct glucuronidation and chiral inversion), it is concluded that CYP2C8 plays a minor role in (*R*)-(-)-IBU (<10%) and (*S*)-(+)-IBU (~13%) clearance. By extension, one would not expect CYP2C8 inhibition (and genotype) to greatly impact the PK profile of either enantiomer. On the other hand, CYP2C9 inhibition and genotype is expected to impact the PK of (*S*)-(+)-IBU.

Introduction

There has been continued interest in the safety and ADME properties of cyclooxygenase inhibitors. This has extended to IBU, which is administered as a racemic mixture of (*S*)-(+)- and (*R*)-(-)-enantiomers (Rodrigues, 2005; Blanco et al., 2008; Pilotto et al., 2007; Agundez et al., 2007). The metabolism of both enantiomers is complex and involves direct (acyl) glucuronidation, 2-hydroxylation, and 3-hydroxylation (methyl hydroxylation) (Fig. 1). Once formed, the 3-hydroxy metabolite is metabolized almost completely to the corresponding carboxy derivative via cytosolic dehydrogenases (Rudy et al., 1991; Davies, 1998; Hamman et al., 1997). Only (*R*)-(-)-IBU undergoes (unidirectional) chiral inversion, which is significant because pharmacological activity following a racemic dose is attributed largely to the (*S*)-(+)-enantiomer (Davies, 1998; Hao et al., 2005; Ding et al., 2007). Overall, it appears that P450-dependent metabolism accounts for about 70% and 30% of (*S*)-(+)-IBU and (*R*)-(-)-IBU clearance, respectively (Rodrigues, 2005). At first glance, the PK profile of the latter is expected to be minimally impacted by P450 inhibitors and genotype (e.g., *CYP2C9*1/*3*, *CYP2C9*3/*3*; *CYP2C8*1/*3*, *CYP2C8*3/*3*).

Currently available in vitro data show that CYP2C9 plays a major role (> 70%) in the oxidative metabolism of racemic IBU and its individual enantiomers. However, hydroxylation of both enantiomers has been measured also with rCYP2C8 and other P450s (CYP3A4 and CYP2C19) (Leeman et al., 1993; Hamman et al., 1997; McGinnity et al., 2000). Such data have led various groups to conclude that both CYP2C forms catalyze the oxidative metabolism of IBU and attempts have been made to evaluate the impact of both *CYP2C9* and *CYP2C8* genotype on the PK, pharmacodynamics, and side effect profile of IBU enantiomers (Garcia-Martin et al.,

2004; Martinez et al., 2005; Kirchheiner et al., 2002; Blanco et al., 2008; Pilotto et al., 2007). Clinical drug interaction studies with known inhibitors of CYP2C9 (e.g., fluconazole) and CYP2C8 (e.g., gemfibrozil) have been conducted also (Tornio et al., 2007; Hynninen et al., 2006).

It is worth noting, however, that CYP2C8-selective chemical inhibitors and inhibitory Mabs were not available when Hamman et al. (1997) conducted their in vitro P450 reaction phenotyping study. Therefore, the CYP2C8-catalyzed 2- and 3-hydroxylation of individual IBU enantiomers in HLM warranted further study and the role of CYP2C9 and CYP2C8 therein was assessed using available selective inhibitors of each P450 form (chemicals and antibodies). Both enantiomers were incubated with a panel of recombinant human P450s also and the data were compared to the inhibition profile obtained with HLM. Throughout the present study, a wide range of (*S*)-(+)-IBU and (*R*)-(-)-IBU concentrations was employed (1 to 500 μM). Such a range encompasses the clinically relevant free (~ 1 μM) and total (~100 μM) plasma concentrations of each enantiomer (Andersson et al., 2004; Davies, 1998; Takanohashi et al., 2007). Integration of the above in vitro data, with known human ADME information, may help rationalize reports describing IBU-P450 inhibitor combinations and IBU PK-P450 genotype associations (Garcia-Martin et al., 2004; Martinez et al., 2005; Kirchheiner et al., 2002; Tornio et al., 2007; Hynninen et al., 2006; Bell et al., 2007).

DMD Fast Forward. Published on September 11, 2008 as DOI: 10.1124/dmd.108.022970
This article has not been copyedited and formatted. The final version may differ from this version.

Materials and Methods

Materials. (*S*)-(+) and (*R*)-(-) enantiomers of IBU [2-(4-isobutylphenyl)propionic acid] were purchased from BIOMOL Research Labs, Inc (Plymouth Meeting, PA). 2-OH (racemic) authentic standard and 3-carboxy IBU (racemate for synthesis of 3-OH) were obtained from Toronto Research Chemicals (North York, Ontario, Canada). Sulfaphenazole and 7-hydroxycoumarin (internal standard) were purchased from Sigma-Aldrich (St Louis, MO). Montelukast was obtained from a commercial source also (Sequoia Research Products, Pangbourne, UK). Ascites fluid containing Mabs selective for CYP2C8 (preparation 281-1-1), CYP2C9 (preparation 763-15-5) and hen egg white lysozyme (preparation HyHel-9) were purchased by special order from the Laboratory of Molecular Carcinogenesis and Laboratory of Metabolism (National Cancer Institute, National Institutes of Health, Bethesda, MD). Pooled HLM (n = 27 different organ donors) and baculovirus-infected insect cell microsomes (Supersomes®) containing various cDNA-expressed human P450s (co-expressed with P450 oxidoreductase) were purchased from BD Gentest (Woburn, MA). HLM preparations from 12 individual (*CYP2C9* and *CYP2C8* genotyped) organ donors were purchased by special order from BD Gentest also. All HLM preparations were characterized in terms of total P450, cytochrome c reductase activity, diclofenac 4'-hydroxylation (CYP2C9), paclitaxel 6α-hydroxylase (CYP2C8), and testosterone 6β-hydroxylase (CYP3A) activity. All other reagents and chemicals were of analytical grade and highest quality available commercially.

3-OH Synthesis, Isolation and Structure Confirmation. *Synthesis.* 3-OH was synthesized using a three-step procedure. First, 3-carboxy-IBU [3-(4-(1-carboxyethyl)phenyl)-2-

methylpropanoic acid; 35 mg, 0.148 mmol] was dissolved in ethanol (5 mL). The solution was refluxed for 2.5 hr following the addition of 1 drop of sulfuric acid. After the reaction was completed, the reaction solvent was removed under reduced pressure and the residue was diluted with dichloromethane and saturated sodium bicarbonate aqueous solution. The product was extracted with dichloromethane twice (2 x 15 mL), dried over sodium sulfate and concentrated to dryness to give the di-ester as a white solid (40 mg, 92% yield; *m/z* = 315.35 [M + 23]).

Second, the di-ester (40 mg, 0.137 mmol) was dissolved in THF and 1M $LiAlH_4$ (in THF) was added dropwise at room temperature. After the addition of 45 drops of $LiAlH_4$ (0.6 mL, 0.6 mmol), HPLC (at 220 nm) showed that the ratio of diol [3-(4-(1-hydroxypropan-2-yl)phenyl)-2-methylpropan-1-ol], mono-esters [ethyl 2-(4-(3-hydroxy-2-methylpropyl)phenyl)-propanoate and ethyl 3-(4-(1-hydroxypropan-2-yl)phenyl)-2-methylpropanoate], and starting di-ester was 5 : 3 : 2.5. The reaction was quenched with 1N HCl and extracted with dichloromethane. The organic layer was concentrated under reduced pressure and then the residue was purified by flash chromatography to give a mixture of the mono-esters as white solids, which could not be separated by column chromatography (*m/z* = 273.35 [M + 23]).

Third, the mixture of the mono-esters was dissolved in methanol (2 mL) and 2 drops of 50 wt% sodium hydroxide aqueous solution and water (1 mL) was added. The solution was stirred at room temperature for 2 hr, then acidified with 1N HCl to pH < 4, and the resulting products were extracted with dichloromethane (2 x 10 mL). The organic layer was dried over sodium sulfate and concentrated to dryness to give 2-(4-(3-hydroxy-2-methylpropyl)phenyl)-propanoic acid (3-OH) and 3-(4-(1-hydroxypropan-2-yl)phenyl)-2-methylpropanoic acid (8 mg, 0.035 mmol; *m/z* = 221.20 [M – 1]).

Isolation. The residue containing 3-OH and 3-(4-(1-hydroxypropan-2-yl)phenyl)-2-methylpropanoic acid (isomer) was dissolved in 0.8 mL of methanol. The methanol solution was subjected to semi-preparative HPLC; column, YMC ProC_{18} 20 x 150 mm, S5 (Waters Corporation, Milford, MA); mobile phase, 0.1% formic acid in water (A) / 0.1% formic acid in Acetonitrile (B); gradient, 10% to 27% B in 5 min, 27% B for 30 min. The flow rate was 10 mL/min with UV detection at 220 nm. Under these conditions, 3-OH and the isomer eluted at approximately 24 and 22 min, respectively. Fractions containing 3-OH and the isomer were pooled separately and lyophilized. After lyophilization, 3-OH (0.5 mg) and isomer (3 mg) were obtained as white powder and the former was submitted for NMR analysis.

Structure confirmation. NMR data were collected on a JEOL Eclipse NMR spectrometer operating at 500.16 MHz resonance frequency and fitted with a 5 mm auto tune Z-gradient broadband probe. Samples (0.5 mg) of the reputed 3-OH and undesired synthetic isomer (3.0 mg) were each dissolved in 180 μL of 99.95% d_4-methanol (Cambridge Isotope Laboratories, Inc, Andover, MA) and placed in a 3 mm NMR tube. One and two dimensional ^{1}H and ^{13}C NMR experiments (^{1}H, ^{13}C, DEPT-135, COSY, ^{1}H-^{13}C-HMQC, ^{1}H-^{13}C-HMBC) were performed on both samples. The complete ^{1}H and ^{13}C chemical shift assignment was accomplished by detailed analysis of the correlated spectra. The relative and absolute stereochemistry of the two chiral centers was not confirmed.

For 3-OH, the complete ^{1}H-^{1}H spin coupling systems of the 3-hydroxy-2-methylpropyl moiety and propanoic acid moiety were observed in the COSY spectrum. ^{1}H-^{13}C long range correlations from both the doublet methyl (0.86 ppm) and the benzylic methylene protons (2.75 and 2.32 ppm) to the carbon of the terminal hydroxyl methylene group at 68.0 ppm were observed. ^{1}H NMR (500 MHz, *methanol-d_4*) δ ppm 8.46 (1 H, br. s.), 7.22 (2 H, d, *J*=7.7 Hz),

7.12 (2 H, d, *J*=7.7 Hz), 3.66 (1 H, q, *J*=7.2 Hz), 3.42 (1 H, dd, *J*=11.0, 6.0 Hz), 3.36 (1 H, dd, *J*=11.0, 6.6 Hz), 2.75 (1 H, dd, *J*=13.5, 5.8 Hz), 2.32 (1 H, dd, *J*=13.5, 8.5 Hz), 1.86 (1 H, dddd, *J*=14.71, 6.5, 6.3, 6.0 Hz), 1.43 (3 H, d, *J*=7.2 Hz), 0.86 (3 H, d, *J*=6.6 Hz). ^{13}C NMR (126 MHz, *methanol-d*$_4$) δ ppm 179.4 140.9, 140.5, 130.5 (2 C), 128.5 (2 C), 68.0, 47.0, 40.4, 39.3, 19.4, 16.9.

Incubation of IBU Enantiomers with Recombinant P450 Proteins and HLM. Incubations were carried out in 96-well Thermowell Gold plates (Corning Inc., Corning, NY) using an 8-tip Genesis 150 liquid handler (Tecan Group Ltd, Research Triangle Park, NC) equipped with a temperature-controlled shaker. The incubation mixture (final volume of 0.2 mL) at 37°C consisted of the following: 0.1 M potassium phosphate buffer (pH 7.4), $MgCl_2$ (2.5 mM), protein (HLM, 0.05 mg/mL; recombinant P450, 1.25 nmol/mL), and individual IBU enantiomer (1 to 1000 μM) dissolved in acetonitrile (1.0%, v/v, final concentration). Following a 5-min pre-warming, the reaction was started with NADPH (2.4 mM). Routinely, the reaction was terminated at 20 to 30 mins by transferring 120 μL of incubation mixture into a MultiScreen filter plate (Millipore, Billerica, MA) pre-loaded with 240 μL ice-cold acetonitrile containing 7-hydroxycoumarin (1 μM final concentration). All reactions were linear with respect to time and protein (or enzyme) concentration.

For each recombinant P450 form, the normalized rate (NR) was calculated based on the turnover (pmol/min per pmol P450) and the reported specific content of each P450 form in HLM (pmol/mg). The total normalized rate (TNR) was calculated as the sum of the NR values for each P450. For each P450 form, the NR was expressed as a percent of the TNR (Rodrigues,

1999). Representative (mean) specific contents were used for CYP3A4, CYP2E1, CYP2D6, CYP2C19, CYP1A2, CYP2C9, CYP2C8, CYP2B6, and CYP2A6 (108, 49, 10, 19, 45, 96, 64, 39 and 41 pmol/mg, respectively) (Rodrigues, 1999; Zhang et al., 2007; Lapple et al., 2003; Lasker et al., 1998).

Identification and Quantitation of 2-OH and 3-OH. Following the addition of cold acetonitrile to the incubates, the filter plate (above) was stacked with a 2-mL 96-well plate (VWR International, West Chester, PA) preloaded with water (360 μL) then vortexed and centrifuged at 2,000x g (5 minutes). Approximately 10 μL of supernatant was analyzed by LC-MS/MS; API4000 LC-MS/MS tandem mass spectrometer (Applied Biosystems, Ontario, Canada) equipped with an turbo-V source, two LC-10ADvp pumps with a SCL-10ADvp controller and DGU-14 solvent degasser (Shimadzu, Columbia, MD), and a CTC PAL autosampler (LEAP, Carrboro, NC). A Luna phenyl-hexyl column (150 x 2.0 mm; Phenomenex, Torrance, CA) was used to achieve HPLC separation. The column was maintained at room temperature, with a gradient elution at a flow rate of 0.3 mL/min; mobile phase A (0.1% formic acid in water) and B (0.1% formic acid in acetonitrile). 2-OH and 3-OH were chromatographically separated using a gradient of 10 to 60% B (over 5 min) followed by a gradient to 100% B (over 2.5 min). Retention times were approximately 4.3, 4.7 and 4.8 minutes for 7-hydroxycoumarin, 2-OH and 3-OH, respectively. The mass spectrometer was operated under atmospheric pressure ionization, in the negative ion (multiple reaction monitoring) mode. Ion transitions were monitored for 2-OH and 3-OH (*m/z* 221→1770) and 7-hydroxycoumarin (*m/z* 161→133). The product ion scan (*m/z* 110 to 240) for 2-OH and 3-OH (parent *m/z* 221) was obtained in order to confirm the structure of the HLM metabolites found at retention time 4.7 and

4.8 min, respectively. The spectra associated with the metabolite peaks detected in HLM incubates matched the synthesized 3-OH and the commercially available 2-OH authentic standard.

For the two IBU hydroxy metabolites, mass detections were acquired and quantitative analysis was performed using Analyst software version 1.4.2 (Applied Biosystems, Ontario, Canada). In each case, the analyte to 7-hydroxycoumarin peak area ratios of the calibrators were fitted to a quadratic regression model (weighted 1/x). Calibration standards were prepared in HLM and extracted with acetonitrile in the same manner as the samples (above). A 6-point standard curve (0.1 to 2000 nM in duplicate) was set up for 2-OH and was fitted to a quadratic regression model (weighted 1/x; correlation coefficient $\geq$ 0.99). The concentration of 2-OH and 3-OH in each sample was calculated using this 2-OH standard curve. No attempt was made to separate and quantitate the two individual diastereomeric forms of 3-OH (e.g., (*R*),(*S*)-3-OH and (*R*),(*R*)-3-OH).

Kinetic Studies Involving HLM, rCYP2C8 and rCYP2C9. Kinetic parameters describing the 2- and 3-hydroxylation of each IBU enantiomer were determined after incubation with HLM and recombinant P450s as described above. However, a range of individual IBU enantiomer (nominal) concentrations was employed (1, 2, 4, 8, 16, 32, 63, 125, 250, and 500 μM; or 4, 9, 20, 40, 70, 120, 270, 520 and 1000 μM). Rates of 2-hydroxylation and 3-hydroxylation were determined and the untransformed data were analyzed using non-linear methods employing KaleidaGraph 3.6 (Synergy Software, Reading, PA). The data were fit to numerous models (Tracy and Hummel, 2004; Korzekwa et al., 1998; Shou et al., 1999), but only the best fits are reported as judged by visual inspection, coefficient of determination (R^2) and the standard error

DMD Fast Forward. Published on September 11, 2008 as DOI: 10.1124/dmd.108.022970
This article has not been copyedited and formatted. The final version may differ from this version.

(± SE) of the parameter estimate (K_m, V_{max} and CL_{int2}). Data were best described by a single-K_m or two-K_m (biphasic) model (eq. 1, and 2, respectively).

$$v = \frac{V_{max} * [S]}{K_m + [S]} \quad (1)$$

$$v = \left(\frac{V_{max1} * [S]}{K_{m1} + [S]} \right) + CL_{int2} * [S] \quad (2)$$

Inhibition Studies. Inhibition studies with P450 form-selective chemical inhibitors were carried out as described above, at a final IBU enantiomer concentration of 1, 20, and 500 μM. In this instance, HLM preparations (0.05 mg/mL) were co-incubated with solvent only (acetonitrile, 1.0%, v/v), sulfaphenazole (5 or 10 μM, CYP2C9 inhibitor), or montelukast (0.2 or 0.4 μM, CYP2C8 inhibitor). Inhibitor concentrations were chosen on the basis of published P450 form-selectivity data and available information related to inhibition constants (Rodrigues, 1999; Zhang et al., 2007; Walsky et al., 2005a, 2005b; Ha-Duong et al., 2001).

Mouse ascites fluid, containing Mabs (anti-CYP2C9, anti-CYP2C8 or anti-hen egg white lysozyme), was diluted with assay buffer and then added to HLM as described by Krausz et al., (2001). The effect of each Mab preparation on the rates of IBU enantiomer (1, 20 or 500 μM) hydroxylation was then determined using the assay conditions described above. All inhibition data are represented as percent inhibition (versus solvent alone control or control Mab) (eq. 1);

$$\% \text{ inhibition} = [(v_o - v_i)/v_o] * 100 \quad (1)$$

where v_o is the rate of reaction in the presence of solvent only (or control Mab) and v_i is the rate of reaction in the presence of the chemical inhibitor (or anti-P450 Mab).

Results

Kinetics of IBU Hydroxylation. In the present study, a sensitive LC-MS/MS method was developed to measure the 2- and 3-hydroxylation of (*S*)-(+)-IBU and (*R*)-(-)-IBU after incubation with HLM and recombinant P450s. It was possible to measure metabolite formation under linear conditions (incubation time and protein concentration) and determine K_m and V_{max}. Overall, the kinetic parameters shown in Table 1 were found to be more or less similar to those reported by Hamman et al (1997). Except for the 3-hydroxylation of (*R*)-(-)-IBU catalyzed by HLM (K_m ~ 120 μM), and 2-hydroxylation catalyzed by rCYP2C8 (K_m ~ 280 μM), the data were described by two-K_m Michaelis-Menten kinetics and there was no evidence for autoactivation or substrate inhibition (Tracy and Hummel, 2004; Korzekwa et al., 1998; Shou et al., 1999). In the presence of HLM, formation of 3-OH was favored over 2-OH (CL_{int1} ratio ~3), which is expected because the recovery ratio [(3-OH + 3-carboxy-IBU)/2-OH] of (*S*)-(+)-IBU and (*R*)-(-)-IBU metabolites in human excreta is greater than unity (Rudy et al., 1991; Davies, 1998; Rodrigues, 2005). For rCYP2C8, the rates of IBU 3-hydroxylation were too low to permit kinetic analyses.

Metabolism of IBU Enantiomers in the Presence of Recombinant P450s. IBU enantiomers (1 μM) were also incubated with a panel of recombinant human P450s and appreciable rates of 2- and 3-hydroxylation were measured only with rCYP2C9 [(*S*)-(+)-IBU, 0.15 and 0.32 pmol/min per pmol P450; (*R*)-(-)-IBU, 0.11 and 0.17 pmol/min per pmol P450, respectively]. At a higher concentration of each IBU enantiomer (500 μM), however, additional P450s were shown to catalyze 3-hydroxylation (CYP2C19) and 2-hydroxylation (CYP2C8, CYP3A4, CYP2C19, CYP2E1 and CYP2B6) (Fig. 2). For both enantiomers, rCYP2C9 demonstrated less

regio-selectivity (2-OH versus 3-OH formation) when compared to other P450s such as rCYP2C8, rCYP3A4, and rCYP2C19. Normalization of turnover, in terms of average P450 isozyme expression in HLM, confirmed that CYP2C9 plays a major role (~90%) in 3-hydroxylation, and that CYP2C9 (~35%), CYP3A4 (~40%), CYP2C8 (~10%), and CYP2C19 (~7%) are all expected to contribute to 2-OH formation in HLM (Fig. 2).

Assessment of the P450s Involved in IBU Hydroxylation in Pooled HLM. Prior to conducting studies with the IBU enantiomers, the anti-CYP2C9 and anti-CYP2C8 Mab preparations employed as reaction phenotyping tools were characterized in terms of their ability to inhibit the requisite probe activities in HLM. Under the assay conditions chosen, anti-CYP2C9 and anti-CYP2C8 were able to inhibit (~80% maximal inhibition) the CYP2C9-dependent 4'-hydroxylation of diclofenac (10 μM) and CYP2C8-dependent 6α-hydroxylation of paclitaxel (5 μM) in pooled HLM, respectively. Some inhibition (3%) of diclofenac 4'-hydroxylase activity was observed with the anti-CYP2C8 Mab preparation. No inhibition of paclitaxel 6α-hydroxylation was observed with the anti-CYP2C9 Mab preparation.

In the present study, sulfaphenazole and anti-CYP2C9 Mabs were used as selective inhibitors of CYP2C9 and caused marked inhibition (≥73%) of (*S*)-(+)-IBU and (*R*)-(-)-IBU (1 and 20 μM) 2- and 3-hydroxylation in pooled HLM (Fig. 3 and 4). Furthermore, 2-hydroxylation and 3-hydroxylation of both IBU enantiomers (20 μM) was highly correlated with diclofenac 4'-hydroxylation in a bank of HLM (correlation coefficient ranging from 0.89 to 0.93; n = 15 livers). Correlations of both IBU hydroxylation reactions with activities selective for other

P450s (e.g., paclitaxel 6α-hydroxylase, testosterone 6β-hydroxylase, and (*S*)-mephenytoin 4'-hydroxylase) were weak (correlation coefficient < 0.62) (data not shown). Overall, the data indicated that CYP2C9 plays a major role at lower concentrations of (*S*)-(+)-IBU and (*R*)-(-)-IBU (≤ 20 μM). In agreement, less inhibition (≤25%) was observed when montelukast and anti-CYP2C8 Mabs were added to the preparation of pooled HLM (Fig 3 and 4).

The P450 reaction phenotype of both IBU enantiomers was more complex at the higher concentration of substrate (500 μM). Although the 3-hydroxylation of (*S*)-(+)-IBU and (*R*)-(-)-IBU was markedly inhibited by sulfaphenazole and anti-CYP2C9 MAbs (66 to 83% and 70 to 77%, respectively), the two inhibitors elicited less of an effect (30 to 47% inhibition) on the 2-hydroxylation reaction (Fig. 3 and 4). These results indicated that CYP2C9-dependent 2-hydroxylation in pooled HLM is decreased at higher IBU concentrations. CYP2C8 does not account for all of the remaining 2-hydroxylation activity therein, because montelukast and anti-CYP2C8 MAbs failed to inhibit both reactions more than ~20% (Fig 3 and 4). With the recombinant P450 data as a guide (Fig. 2), additional inhibition studies were conducted with ketoconazole (1 μM) and (+)-*N*-3-benzyl-nirvanol (1 μM). The two are known to be selective inhibitors of CYP3A4 and CYP2C19 in HLM, respectively (Suzuki et al., 2002; Zhang et al., 2007; Walsky et al., 2005b). In the presence of pooled HLM, ketoconazole was able to inhibit the 2- and 3-hydroxylation of (*S*)-(+)-IBU (33 ± 2.2% and 11 ± 1.4%, respectively) and (*R*)-(-)-IBU (32 ± 2.5% and 14 ± 2.1%, respectively). Some inhibition of (*S*)-(+)-IBU 2- and 3-hydroxylation (9.0 ± 2.6% and 5.4 ± 1.4%, respectively), and (*R*)-(-)-IBU 2-hydroxylation (5.0 ± 2.5%) was observed with (+)-*N*-3-benzyl-nirvanol.

Additional Reaction Phenotyping with HLM Preparations from *CYP2C8* and *CYP2C9* Genotyped Livers. The CYP reaction phenotyping of both IBU enantiomers (500 μM) was then expanded to include a panel of individual HLM preparations from 12 subjects that were genotyped for *CYP2C8* and *CYP2C9* alleles (Table 2). In all cases, it was possible to evaluate the inhibitory effects of montelukast and sulfaphenazole (Fig. 5). For (*R*)-(-)-IBU, formation of 2-OH was inhibited 14 to 35% (montelukast) and 41 to 64% (sulfaphenazole). Formation of 3-OH was inhibited 5 to 28% (montelukast) and 83 to 89% (sulfaphenazole). The 2- and 3-hydroxylation of (*S*)-(+)-IBU was similarly inhibited by montelukast (15 to 34%; 9 to 17%, respectively) and sulfaphenazole (32 to 52%; 79 to 83%, respectively). Based on the mean inhibition data (across all twelve HLM preparations in the panel), CYP2C9 and CYP2C8 accounted for the majority (>95%) of 3-OH formation. As expected, both P450s together only accounted for ~70% of 2-OH formation. The involvement of CYP3A4 and CYP2C19 is inferred based on the data obtained with pooled HLM. Overall, there appeared to be no obvious correlation between the extent of inhibition and *CYP2C8* (or *CYP2C9*) genotype. Moreover, because of the relatively small number of individual HLM preparations it was not possible to assess the impact of genotype on the rate of IBU hydroxylation.

Discussion

The oxidative metabolism of IBU is complex because of the regio- and stereoselective hydroxylation of its enantiomers (Rudy et al., 1991; Davies, 1998; Hamman et al., 1997). However, such hydroxylation has to be viewed in light of additional clearance pathways (Fig. 1). For example, it has been estimated that an appreciable fraction of (*R*)-(-)-IBU (~60%) metabolism involves unidirectional chiral inversion to the (*S*)-(+)-enantiomer (Davies, 1998). Metabolism via direct glucuronidation (9%), in addition to 2-hydroxylation (10%), and 3-hydroxylation (20%), has been reported also (Rudy et al., 1991; Davies, 1998). In contrast, the (*S*)-(+)-enantiomer of IBU undergoes no detectable chiral inversion and undergoes direct glucuronidation (14%), 2-hydroxylation (28%), and 3-hydroxylation (45%) (Rudy et al., 1991; Davies, 1998; Rodrigues, 2005). Therefore, P450-mediated clearance is more important for the (*S*)-(+)-enantiomer (~70% versus ~30%).

Although the in vitro P450-dependent metabolism of racemic IBU (and its enantiomers) has been documented, the contributions of individual P450s (beyond CYP2C9) in HLM preparations have not been described (Leeman et al., 1993; Hamman et al., 1997; McGinnity et al., 2000). Therefore, additional studies were warranted given the number of reports describing IBU-P450 inhibitor combinations and IBU PK-P450 genotype associations (Garcia-Martin et al., 2004; Martinez et al., 2005; Kirchheiner et al., 2002; Tornio et al., 2007; Hynninen et al., 2006; Bell et al., 2007). Towards this end, an LC-MS/MS assay was developed to monitor the formation of both 2-OH and 3-OH in vitro. The assay enabled assessment of metabolite formation in the presence of HLM and recombinant P450s under linear conditions. It was possible to evaluate the kinetics of IBU enantiomer hydroxylation, determine K_m and V_{max} for

HLM, rCYP2C9 and rCYP2C8, and confirm the biphasic (two-K_m) kinetics described by Hamman et al. (1997). Such a profile may result from two populations of P450s (low K_m and high K_m), or the binding of substrate to two sites on a single (dominant) P450 (Tracy and Hummel, 2004; Korzekwa et al., 1998). CYP2C9 is a candidate for the latter scenario, because the enzyme in recombinant form is known to exhibit biphasic kinetics (Tracy et al., 2002; Hamman et al., 1997). This was confirmed with rCYP2C9 (Table 1).

It has been reported that CYP2C9 is a major hydroxylase when HLM are incubated with racemic IBU and its individual enantiomers (Leemann et al., 1993; Hamman et al., 1997). The data described herein are consistent with CYP2C9 playing a major role in 2-OH and 3-OH formation at low concentrations of IBU (≤ 20 μM). However, CYP2C8 is a second CYP2C subfamily member that has been associated with IBU hydroxylation in vitro, although its exact contribution in HLM has not been reported (Hamman et al., 1997). Moreover, in vitro P450 reaction phenotype data for both IBU enantiomers over a wide substrate concentration range are not available. Such information is important and may help reconcile the results of clinical drug interaction studies involving IBU enantiomers. For example, gemfibrozil, a known CYP2C8 inhibitor (Ogilvie et al., 2006; references therein), has been shown to increase the AUC of (*R*)-(-)-IBU up to 1.6-fold (mean, 1.3-fold) in human subjects (Tornio et al., 2007). In the same study, the effect on the AUC of the IBU (*S*)-(+)-enantiomer was not statistically significant. Conversely, fluconazole (CYP2C9 inhibitor) increases (*S*)-(+)-IBU AUC up to 1.9-fold, while having no effect on the AUC of (*R*)-(-)-IBU (Hynninen et al., 2006). Based on such data, one could argue that CYP2C8 and CYP2C9 play a significant role in the clearance of (*R*)-(-)-IBU and (*S*)-(+)-IBU, respectively. This conclusion is consistent with the results of Kirchheiner et al. (2002). The authors were able to show that the AUC of (*S*)-(+)-IBU was increased (1.7-fold) in

subjects genotyped *CYP2C9*3/*3* (versus *CYP2C9*1/*1*); with no effect on (*R*)-(-)-IBU AUC. The impact of *CYP2C8* genotype (e.g., *CYP2C8*1/*3* and *CYP2C8*3/*3*) on IBU enantiomer PK is more difficult to interpret (Martinez et al., 2005; Garcia-Martin et al., 2004), because of the linkage between the *CYP2C8*3* and *CYP2C9*2* alleles (Rodrigues, 2005, references therein). CYP2C8 phenotype-genotype associations are further complicated by haplotype (Tornio et al., 2008; Saito et al., 2007; Rodriguez-Antona et al., 2007; Kirchheiner et al., 2006; Parikh et al., 2007). This is a very different scenario to *CYP2C9* genotype, which is clearly linked to reductions in drug clearance (*CYP2C9*3* > *CYP2C9*2*) and can be "phenocopied" with inhibitors such as sulfaphenazole and fluconazole (Rodrigues, 2005; Kirchheiner and Brockmoller, 2005; Gardiner and Begg, 2006).

Despite clinical reports linking CYP2C8 to IBU enantiomer metabolism, especially (*R*)-(-)-IBU (Tornio et al., 2007 Martinez et al., 2005; Garcia-Martin et al., 2004), the data presented herein demonstrate that CYP2C8 plays a relatively minor role in the hydroxylation of both enantiomers. Firstly, minimal hydroxylation of both enantiomers was detected with rCYP2C8 (versus rCYP2C9) at the low substrate concentration (1 μM). Even at the higher IBU concentration of 500 μM, the normalized turnover rates measured with recombinant P450s suggested that the contribution of CYP2C8 was minimal (≤ 11%) (Fig. 2). Second, montelukast and anti-CYP2C8 Mabs were relatively weak (≤ 35%) inhibitors of (*R*)-(-)-IBU and (*S*)-(+)-IBU hydroxylation in pooled HLM (Fig. 3 and 4) and individual HLM (Fig. 5) preparations. Despite such weak inhibition, however, it was possible to discern some preference for 2-hydroxylation (11 to 24% inhibition in pooled HLM; 14 to 35% inhibition for individual HLM) over 3-hydroxylation (3 to 8% inhibition in pooled HLM; 5 to 28% inhibition for individual HLM).

Although additional P450s (e.g., CYP3A4 and CYP2C19) catalyze IBU hydroxylation in HLM, the above observation is consistent with the regio-selective hydroxylation (2-OH/3-OH ratio ~10) observed with rCYP2C8 (Fig. 2).

Collectively, the P450 reaction phenotype data described herein indicated that the respective contributions of CYP2C9, CYP2C8, CYP3A4 and CYP2C19 in HLM are ~45%, ~23%, 33% and 9% (2-hydroxylation of (*S*)-(+)-IBU), ~80%, ~14%, 11%, and ~5% (3-hydroxylation of (*S*)-(+)-IBU), ~50%, ~25%, 32%, and 5% (2-hydroxylation of (*R*)-(-)-IBU), and ~85%, ~17%, 14%, and <2% (3-hydroxylation of (*R*)-(-)-IBU) at a high concentration of IBU (500 μM). Given the known P450 selectivity of sulfaphenazole and the anti-CYP2C9 Mab preparations used, it can be assumed that CYP2C9 plays a major role (75 to 100%) in both hydroxylation reactions at lower concentrations of IBU (≤ 20 μM). At the same low IBU concentrations, the contribution of CYP2C8 is low (≤25%).

When all IBU enantiomer clearance pathways are considered (direct glucuronidation to the acyl glucuronide, chiral inversion, 2-hydroxylation and 3-hydroxylation), and the present reaction phenotype data are integrated across all concentrations of IBU tested, it is calculated that CYP2C9 accounts for 49 to ~70% [(*S*)-(+)-IBU] and 20 to 30% [(*R*)-(-)-IBU] of total clearance. This is consistent with the reported impact of *CYP2C9*3/*3* genotype and fluconazole on (*S*)-(+)-IBU AUC (versus (*R*)-(-)-IBU AUC) (Kirchheiner et al., 2002; Hynninen et al., 2006; Rodrigues, 2005). On the other hand, CYP2C8 contributes to only a small fraction of (*R*)-(-)-IBU (~6%) and (*S*)-(+)-IBU (~13%) clearance. Therefore, (*R*)-(-)-IBU AUC increases of greater than 2-fold in subjects carrying mutant *CYP2C8* alleles are difficult to rationalize based on the in vitro data presented herein and published ADME information (Martinez et al., 2005; Garcia-Martin et

al., 2004; Rodrigues, 2005). The increased (*R*)-(-)-IBU AUC (up to 1.6-fold) with gemfibrozil, in the absence of an effect on (*S*)-(+)-IBU AUC, is also difficult to reconcile with the present data and requires further investigation (Tornio et al., 2007). It is possible that gemfibrozil, a known OATP inhibitor, inhibits the hepatic uptake of IBU enantiomers [(*R*)-(-)-IBU > (*S*)-(+)-IBU]. However, this appears unlikely because neither enantiomer (1 to 500 μM) served as a substrate of human OATP1B1, OATP1B3 and OATP2B1 in vitro (data not shown). Chiral inversion of (*R*)-(-)-IBU to (*S*)-(+)-IBU is an enzyme-catalyzed process and inhibition by gemfibrozil also remains a possibility (Hao et al., 2005). Then again, no inhibition of (*R*)-(-)-IBU chiral inversion was evident in suspensions of primary human hepatocytes co-incubated with gemfibrozil (2 to 200 μM) (data not shown).

Going forward, the CYP2C8-dependent metabolism of IBU enantiomers has to be considered in light of all P450 and non-P450 clearance pathways, and the possible involvement of additional P450s beyond CYP2C8 and CYP2C9 (e.g., CYP2C19 and CYP3A4). In particular, changes in (*R*)-(-)-IBU AUC cannot be ascribed solely to CYP2C8 without regard for possible impact on chiral inversion. Furthermore, one has to take into account the complexities of the CYP2C8 genotype-phenotype relationship. For example, when compared to IBU enantiomers, CYP2C8 plays a significant role in the in vitro metabolism of paclitaxel, repaglinide, amodiaquine, pioglitazone and rosiglitazone. Despite a prominent role in vitro, the impact of *CYP2C8* genotype (e.g., *CYP2C8*3* allele) on the PK of most of the above drugs is not clear (Tornio et al., 2008; Saito et al., 2007; Rodriguez-Antona et al., 2007; Kirchheiner et al., 2006; Parikh et al., 2007). Therefore, the metabolic profile of IBU enantiomers after dosing of subjects carrying different *CYP2C9* and *CYP2C8* alleles requires further study and additional radiolabeled studies may be warranted.

References

Agúndez JA, Martínez C, García-Martín E, Ladero JM (2007) Cytochrome P450 CYP2C9 polymorphism and NSAID-related acute gastrointestinal bleeding. Gastroenterology 133:2071-2072.

Andersson TB, Bredberg E, Ericsson H, Sjoberg H (2004) An evaluation of the in vitro metabolism data for predicting the clearance and drug-drug interaction potential of CYP2C9 substrates. Drug Metab Dispos 32: 715-721.

Bell EC, Ravis WR, Lloyd KB, Stokes TJ (2007) Effects of St. John's wort supplementation on ibuprofen pharmacokinetics. Ann Pharmacother 41:229-234.

Blanco G, Martínez C, Ladero JM, Garcia-Martin E, Taxonera C, Gamito FG, Diaz-Rubio M, Agundez JA (2008) Interaction of CYP2C8 and CYP2C9 genotypes modifies the risk for nonsteroidal anti-inflammatory drugs-related acute gastrointestinal bleeding. Pharmacogenetics 18:37-43.

Davies NM (1998) Clinical pharmacokinetics of ibuprofen. The first 30 years. Clin Pharmacokinet 34: 101–154.

Ding G, Liu Y, Sun J, Takeuchi Y, Toda T, Hayakawa T, Fukushima S, Kishimoto S, Lin W, Inotsume N (2007) Effect of absorption rate on pharmacokinetics of ibuprofen in relation to chiral inversion in humans. J Pharm Pharmacol 59:1509-1513.

Gardiner SJ and Begg EJ (2006) Pharmacogenetics, drug-metabolizing enzymes, and clinical practice. Pharmacol Rev 58: 521-590.

Garcia-Martin E, Martinez C, Tabares B, Frias J, and Agundez JA (2004) Interindividual

variability in ibuprofen pharmacokinetics is related to interaction of cytochrome P450 2C8 and 2C9 amino acid polymorphisms. Clin Pharmacol Ther 76: 119–127.

Ha-Duong NT, Marques-Soares C, Dijols S, Sari MA, Dansette PM, Mansuy D (2001) Interaction of new sulfaphenazole derivatives with human liver cytochrome P450 2Cs: structural determinants required for selective recognition by CYP2C9 and for inhibition of human CYP2Cs. Arch Biochem Biophys 394: 189-200.

Hamman MA, Thompson GA, and Hall SD (1997) Regioselective and stereoselective metabolism of ibuprofen by human cytochrome P450 2C. Biochem Pharmacol 54: 33–41.

Hao H, Wang G, and Sun J (2005) Enantioselective pharmacokinetics of ibuprofen and involved mechanisms. Drug Metab Rev 37: 215–234.

Hynninen VV, Olkkola KT, Leino K, Lundgren S, Neuvonen PJ, Rane A, Valtonen M, Vyyryläinen H, Laine K (2006) Effects of the antifungals voriconazole and fluconazole on the pharmacokinetics of *S*-(+)- and *R*-(-)-Ibuprofen. Antimicrob Agents Chemother 50:1967-72.

Kirchheiner J and Brockmoller J (2005) Clinical consequences of cytochrome P450 2C9 polymorphisms. Clin Pharmacol Ther 17: 1-17.

Kirchheiner J, Meineke I, Freytag G, Meisel C, Roots I, and Brockmoller J (2002) Enantiospecific effects of cytochrome P450 2C9 amino acid variants on ibuprofen pharmacokinetics and on the inhibition of cyclooxygenases 1 and 2. Clin Pharmacol Ther 72: 62–75.

Kirchheiner J, Thomas S, Bauer S, Tomalik-Scharte D, Hering U, Doroshyenko O, Jetter A,

Stehle S, Tsahuridu M, Meineke I, Brockmöller J, Fuhr U (2006) Pharmacokinetics and pharmacodynamics of rosiglitazone in relation to CYP2C8 genotype. Clin Pharmacol Ther 80:657-667.

Korsekwa KR, Krishnamachary N, Shou M, Ogai A, Parise RA, Rettie AE, Gonzalez FJ, Tracy TS (1998) Evaluation of atypical cytochrome P450 kinetics with two-substrate models: evidence that multiple substrates can simultaneously bind to cytochrome P450 active sites. Biochemistry 37: 4137-4147.

Krausz KW, Goldfarb I, Buters JT, Yang TJ, Gonzalez FJ, Gelboin HV (2001) Monoclonal antibodies specific and inhibitory to human cytochromes P450 2C8, 2C9, and 2C19. Drug Metab Dispos 29:1410-1423.

Lapple F, von Richter O, Fromm MF, Richter T, Thon KP, Wisser H, Griese EU, Eichelbaum M, and Kivisto KT (2003) Differential expression and function of CYP2C isoforms in human intestine and liver. Pharmacogenetics 13: 565–575.

Lasker JM, Wester MR, Aramsombatdee E, and Raucy JL (1998) Characterization of CYP2C19 and CYP2C9 from human liver: respective roles in microsomal tolbutamide, *S*-mephenytoin and omeprazole hydroxylations. Arch Biochem Biophys 353: 16–28.

Leemann TD, Transon C, Bonnabry P, and Dayer P (1993) A major role for cytochrome P450TB (CYP2C subfamily) in the actions of non-steroidal anti-inflammatory drugs. Drugs Exp Clin Res 19: 189–195.

McGinnity DF, Parker AJ, Soars M, Riley RJ (2000) Automated definition of the enzymology of drug oxidation by the major human drug metabolizing cytochrome P450s. Drug Metab Dispos 28: 1327-1334.

Martinez C, Garcia-Martin E, Blanco G, Gamito FJ, Ladero JM, and Agundez JA (2005) The effect of the cytochrome P450 CYP2C8 polymorphism on the disposition of (*R*)-ibuprofen enantiomer in healthy subjects. Br J Clin Pharmacol 59: 62–69.

Ogilvie BW, Zhang D, Li W, Rodrigues AD, Gipson AE, Holsapple J, Toren P, Parkinson A (2006) Glucuronidation converts gemfibrozil to a potent, metabolism-dependent inhibitor of CYP2C8: implications for drug-drug interactions. Drug Metab Dispos 34:191-197.

Parikh S, Ouedraogo JB, Goldstein JA, Rosenthal PJ, Kroetz DL (2007) Amodiaquine metabolism is impaired by common polymorphisms in CYP2C8: implications for malaria treatment in Africa. Clin Pharmacol Ther 82:197-203.

Pilotto A, Seripa D, Franceschi M, Scarcelli C, Colaizzo D, Grandone E, Niro V, Andriulli A, Leandro G, Di Mario F, Dallapiccola B (2007) Genetic susceptibility to nonsteroidal anti-inflammatory drug-related gastroduodenal bleeding: role of cytochrome P450 2C9 polymorphisms. Gastroenterology 133:465-71.

Rodrigues AD (1999) Integrated cytochrome P450 reaction phenotyping: attempting to bridge the gap between cDNA-expressed cytochromes P450 and native human liver microsomes. Biochem Pharmacol 57:465-480.

Rodrigues AD (2005) Impact of CYP2C9 genotype on pharmacokinetics: are all cyclooxygenase inhibitors the same? Drug Metab Dispos 33: 1567-1575.

Rodríguez-Antona C, Niemi M, Backman JT, Kajosaari LI, Neuvonen PJ, Robledo M, Ingelman-Sundberg M (2008) Characterization of novel CYP2C8 haplotypes and their contribution to paclitaxel and repaglinide metabolism. Pharmacogenomics J 8:268-277.

Rudy AC, Knight PM, Brater DC, and Hall SD (1991) Stereoselective metabolism of ibuprofen in humans: administration of R-, S- and racemic ibuprofen. J Pharmacol Exp Ther 259: 1133–1139.

Saito Y, Katori N, Soyama A, Nakajima Y, Yoshitani T, Kim SR, Fukushima-Uesaka H, Kurose K, Kaniwa N, Ozawa S, Kamatani N, Komamura K, Kamakura S, Kitakaze M, Tomoike H, Sugai K, Minami N, Kimura H, Goto Y, Minami H, Yoshida T, Kunitoh H, Ohe Y, Yamamoto N, Tamura T, Saijo N, Sawada J (2007) CYP2C8 haplotype structures and their influence on pharmacokinetics of paclitaxel in a Japanese population. Pharmacogenet Genomics 17:461-471.

Shou M, Mei Q, Ettore MW, Dai R, Baillie TA, Rushmore TH (1999) Sigmoidal kinetic model for two co-operative substrate-binding sites in a cytochrome P450 3A4 active site: an example of the metabolism of diazepam and its derivatives. Biochem J 340: 845-853.

Suzuki H, Kneller MB, Haining RL, Trager WF, Rettie AE (2002) (+)-*N*-3-Benzyl-Nirvanol and (-)-*N*-3-Benzyl-Phenobarbital: New Potent and Selective in Vitro Inhibitors of CYP2C19. Drug Metab Dispos 30: 235-239.

Takanohashi T, Koizumi T, Mihara R, Okudaira K (2007) Prediction of the metabolic interaction of netaglinide with other drugs based on in vitro studies. Drug Metab Pharmacokin 22: 409-418.

Tornio A, Niemi M, Neuvonen PJ, Backman JT (2007) Stereoselective interaction between the CYP2C8 inhibitor gemfibrozil and racemic ibuprofen. Eur J Clin Pharmacol 63: 463-469.

Tornio A, Niemi M, Neuvonen PJ, Backman JT (2008) Trimethoprim and the CYP2C8*3 allele have opposite effects on the pharmacokinetics of pioglitazone. Drug Metab Dispos 36:73-80.

Tracy TS and Hummel MA (2004) Modeling kinetic data from in vitro drug metabolism enzyme experiments. Drug Metab Rev 36: 231-242.

Tracy TS, Hutzler JM, Haining RL, Rettie AE, Hummel MA, Dickmann LJ (2002) Polymorphic variants (CYP2C9*3 and CYP2C9*5) and the F114L active site mutation of CYP2C9: effect of atypical kinetic metabolism profiles. Drug Metab Dispos 30: 385-390.

Walsky RL, Obach RS, Gaman EA, Gleeson JP, Proctor WR (2005a) Selective inhibition of human cytochrome P4502C8 by montelukast. Drug Metab Dispos 33:413-418.

Walsky RL, Gaman EA, Obach RS (2005b) Examination of 209 drugs for inhibition of cytochrome P450 2C8. J Clin Pharmacol 45: 68-78.

Zhang H, Davis CD, Sinz MW, Rodrigues AD (2007) Cytochrome P450 reaction-phenotyping: an industrial perspective. Expert Opin Drug Metab Toxicol 3: 667-687.

Footnotes

The authors would like to thank Dr. Yong-Hae Han (Bristol-Myers Squibb, Princeton, NJ) for conducting the in vitro OATP (transport) studies employing HEK-293 cells expressing individual human OATPs (Invitrogen, Carlsbad, CA) described in the *Discussion*. Dr. Yong-Hae Han also conducted the human primary hepatocyte studies (cells obtained from BD Biosciences, San Jose, CA) to evaluate the chiral inversion of (*R*)-ibuprofen. Dr. Yingru Zhang (Bristol-Myers Squibb, Princeton, NJ) is acknowledged for developing LC-MS/MS method for IBU enantiomer chiral analysis (chiral inversion study described in the *Discussion*).

Figure Legends

Fig.1. Primary biotransformation pathways of IBU enantiomers.

*For each IBU enantiomer, the diastereomeric forms of 3-OH (e.g., (*R*),(*S*)- and (*R*),(*R*)-3-OH) and 3-carboxy-IBU are not represented.

Fig. 2. Hydroxylation of IBU enantiomers in the presence of human recombinant P450 proteins.

Both (a) (*S*)-(+)-IBU and (b) (*R*)-(-)-IBU (500 μM) were individually incubated with various recombinant human P450 proteins and the rates of 2-hydroxylation (2-OH) and 3-hydroxylation (3-OH) were measured. Data are expressed as pmol/min per pmol P450. As described in *Materials and Methods*, %TNR represents "percent of total normalized rate" (Rodrigues, 1999).

Fig. 3. Effects of chemical inhibitors and inhibitory antibodies on the hydroxylation of (*S*)-(+)-IBU in the presence of pooled HLM.

(*S*)-(+)-IBU (1, 20 and 500 μM) was incubated with pooled HLM (0.05 mg/mL; n = 27 organ donors) in the presence of solvent alone (acetonitrile, 1.0% v/v), sulfaphenazole (5 or 10 μM), or montelukast (0.2 or 0.4 μM). The two compounds served as putative inhibitors of CYP2C9 and CYP2C8, respectively. (*S*)-(+)-IBU was similarly incubated in the presence of control Mabs (anti-hen egg white lysozyme), anti-CYP2C8 Mabs, or anti-CYP2C9 Mabs (5 μL diluted ascites fluid per incubation). The 2-hydroxylation (2-OH) (a) and 3-hydroxylation (3-OH) (b) of (*S*)-(+)-IBU was determined. Data are presented as the mean (± SD) of three determinations

and are expressed as percent inhibition versus solvent alone (chemical inhibitors) or egg white lysozyme Mab (anti-CYP2C9 and anti-CYP2C8 MAb). See *Materials and Methods*.

Fig. 4. Effects of chemical inhibitors and inhibitory antibodies on the hydroxylation of (*R*)-(-)-IBU in the presence of pooled HLM. See legend to Figure 3, except that the (*R*)-(-)-enantiomer of IBU was incubated with HLM.

Fig. 5. Effect of sulfaphenazole and montelukast on IBU enantiomer 2- and 3-hydroxylation catalyzed by HLM preparations from individual organ donors.

(a) (*R*)-(-)-IBU and (b) (*S*)-(+)-IBU (500 μM) were individually incubated with HLM (0.05 mg/mL) in the presence of sulfaphenazole (10 μM) or montelukast (0.4 μM). For each HLM preparation, data are reported as percent inhibition (versus solvent alone) and represent the mean of duplicate determinations. Duplicates did not vary by more than 10%. For each HLM preparation, control activities (solvent alone) and genotype are presented in Table 2. The mean (±SD) inhibition for each reaction (across all twelve HLM preparations in the panel) is shown.

TABLE 1

Kinetic data describing the 2- and 3-hydroxylation of IBU enantiomers in the presence of rCYP2C8, rCYP2C9 and pooled HLM

Preparation	Substrate	Product	Model	K_m (μM)	SE	V_{max} (pmol/min.mg^{-1})	SE	CL_{int1} (μL/min.mg^{-1})	CL_{int2} (μL/min.mg^{-1})	SE	R^2
HLM	(*S*)-(+)-IBU	2-OH	Biphasic	76	11	233	17	3.07	27	17	0.998
		3-OH	Biphasic	45	5.0	437	19.9	9.71	57	23	0.998
	(*R*)-(-)-IBU	2-OH	Biphasic	125	24	366	41	2.93	29	35	0.988
		3-OH	Single-K_m	115	13	994	35	8.64			0.996
				K_m (μM)	SE	V_{max} (pmol/min.pmol^{-1})	SE	CL_{int1} (μL/min.pmol^{-1})	CL_{int2} (μL/min.pmol^{-1})	SE	
rCYP2C9	(*S*)-(+)-IBU	2-OH	Biphasic	29	4.8	16	1.2	552	10	2.7	0.998
		3-OH	Biphasic	40	4.0	29	2.5	725	28	5.4	0.998
	(*R*)-(-)-IBU	2-OH	Biphasic	45	8.6	17	1.8	378	17	3.0	
		3-OH	Biphasic	46	11	29	3.7	630	33	7.0	0.998
rCYP2C8	(*S*)-(+)-IBU	2-OH	Biphasic	292	54	5.4	1.1	18	2.2	0.91	0.999
	(*R*)-(-)-IBU	2-OH	Single-K_m	282	52	9.4	0.9	33			0.995

Estimates of K_m and V_{max} were determined graphically (see *Materials and Methods*). Data were fitted to a single-K_m or two-K_m (biphasic) model. SE and R^2 represent the standard error of the parameter estimate and coefficient of determination, respectively. CL_{int1} is the ratio V_{max}/K_m and describes the low K_m (K_{m1}) and V_{max1} component. It was not possible to determine the K_m and V_{max} (K_{m2} and V_{max2}) of the second component in the two-K_m model (K_{m2} > 500 μM). However, it was possible to estimate the ratio of the two parameters (CL_{int2}). For rCYP2C8, the rates of IBU 3-hydroxylation were too low to permit kinetic analyses. rCYP2C9 and

rCYP2C8 are the wild type (*1 allele) forms of each enzyme. HLM, pooled human liver microsomes from n = 27 different organ donors.

TABLE 2

IBU enantiomer 2- and 3-hydroxylation, diclofenac 4-hydroxylation (CYP2C9) and paclitaxel 6α-hydroxylation (CYP2C8) activity in HLM preparations from individual genotyped organ donors

	Genotype		(*R*)-(-)-IBU		(*S*)-(+)-IBU		Diclofenac	Paclitaxel
			2-OH	3-OH	2-OH	3-OH	4-Hydroxylase	6α-Hydroxylase
HLM	*CYP2C9*	*CYP2C8*	(pmol/min/mg)	(pmol/min/mg)	(pmol/min/mg)	(pmol/min/mg)	(pmol/min/mg)	(pmol/min/mg)
HH40	*1/*1	*1/*1	168	170	121	163	243	76
HH125	*1/*1	*1/*1	187	115	143	112	183	299
HH55	*1/*1	*1/*1	254	201	181	185	288	396
4532891	*1/*1	*1/*1	206	189	146	186	281	250
4543196	*1/*1	*1/*1	215	212	146	203	287	200
4544547	*1/*1	*1/*3	202	185	130	163	266	250
HH85	*1/*2	*1/*3	157	135	104	121	199	52
4522807	*1/*2	*1/*3	312	318	186	252	410	207
HH131	*1/*2	*1/*3	224	147	142	129	206	237
HH69	*2/*2	*3/*3	94	66	62	54	164	42
4532926	*2/*2	*3/*3	203	181	132	163	277	247
4538092	*2/*3	*1/*3	169	110	126	116	211	111

IBU enantiomer hydroxylation was measured in HLM as described in *Materials and Methods*. Data represent mean of duplicate determinations, which did not vary by more than 10%. The final concentration of each IBU enantiomer was 500 μM. For each HLM preparation, genotype, diclofenac hydroxylase and paclitaxel hydroxylase activities were provided by the supplier (BD Gentest, Wobur)

Figure 1

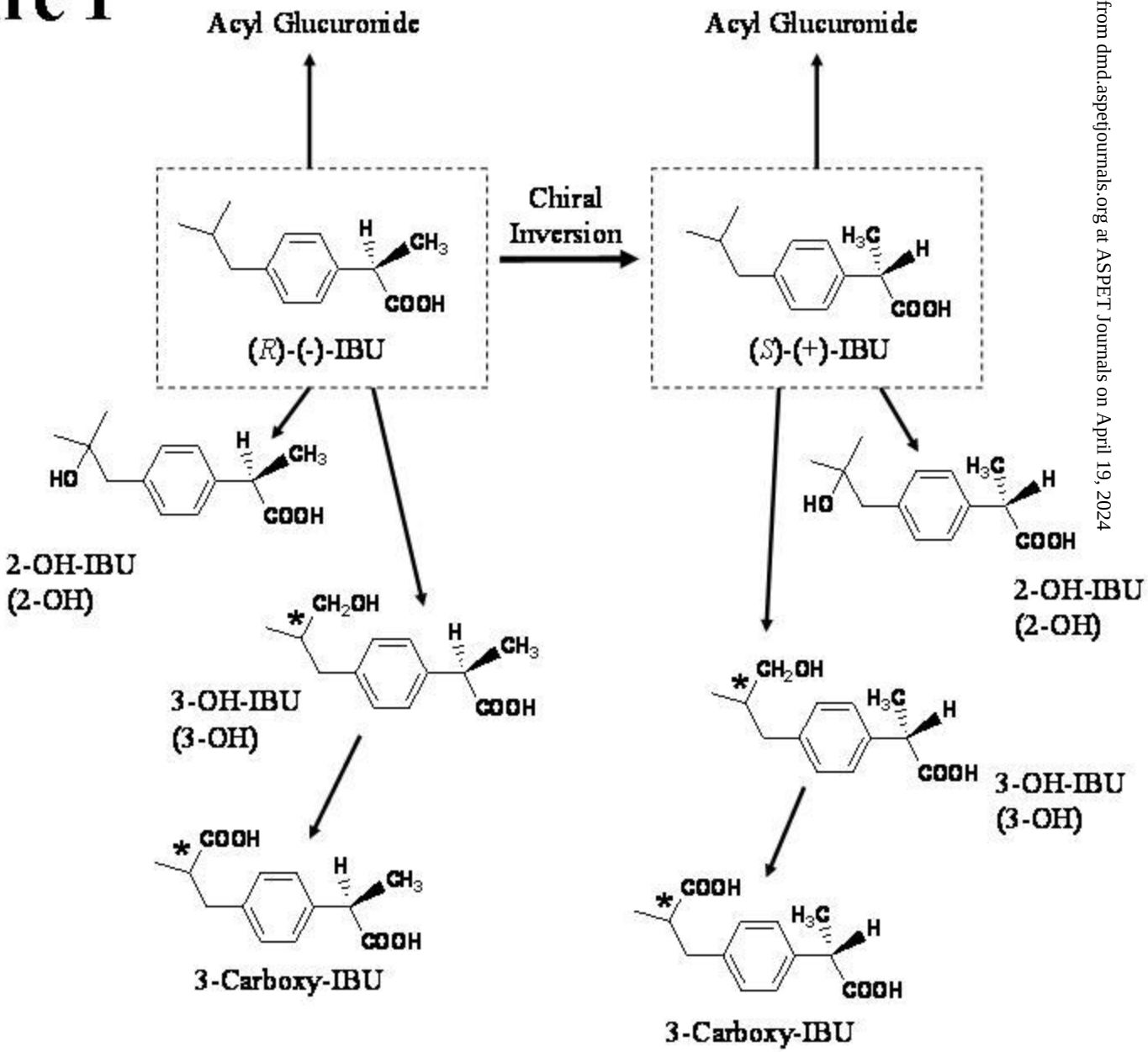

Figure 2A

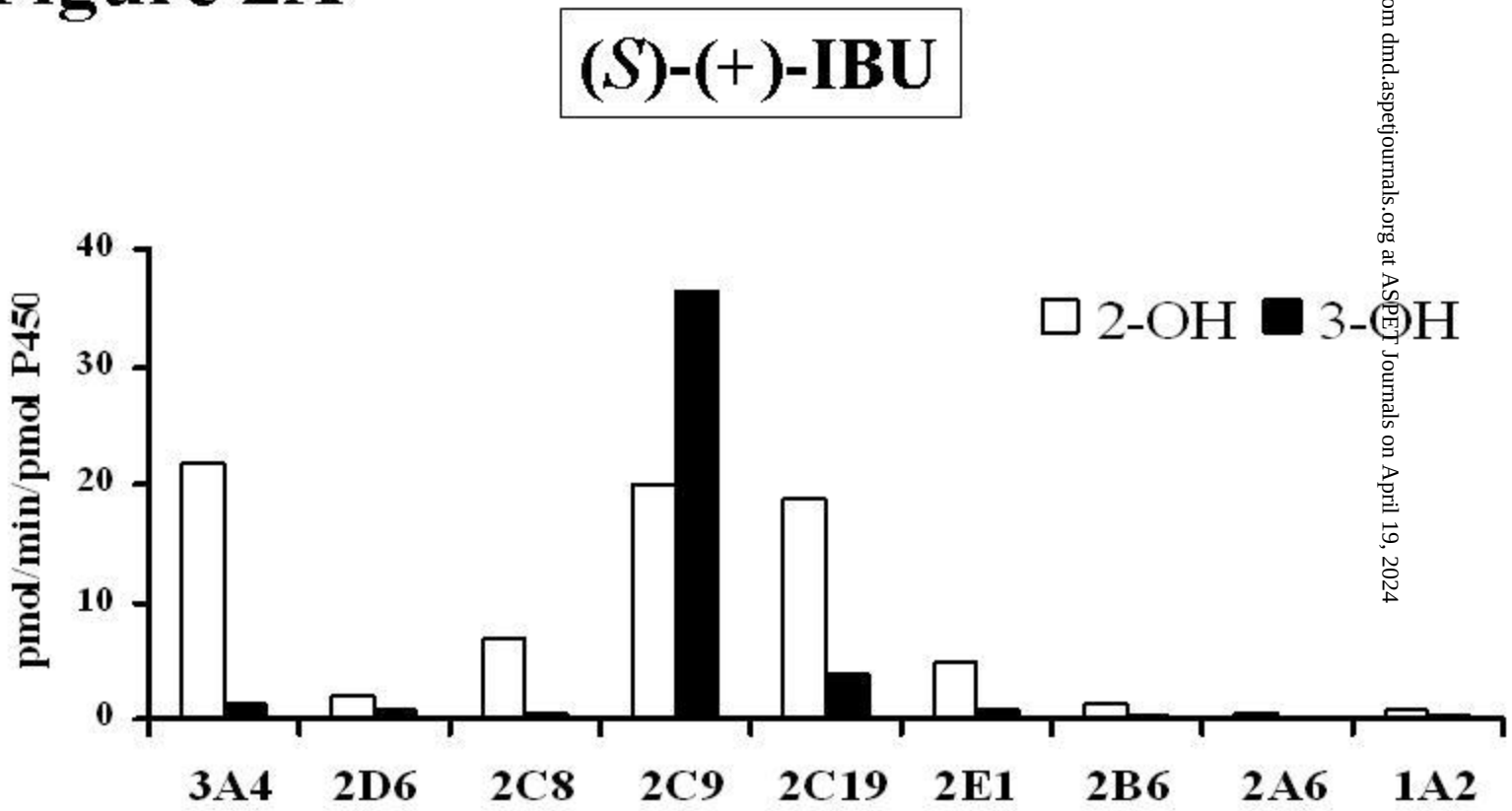

Reaction	%TNR For Each P450 Form								
	3A4	2D6	2C8	2C9	2C19	2E1	2B6	2A6	1A2
2-OH	43	<1	8	35	7	4	<1	<1	<1
3-OH	4	<1	<1	92	2	<1	<1	<1	<1

Figure 2B

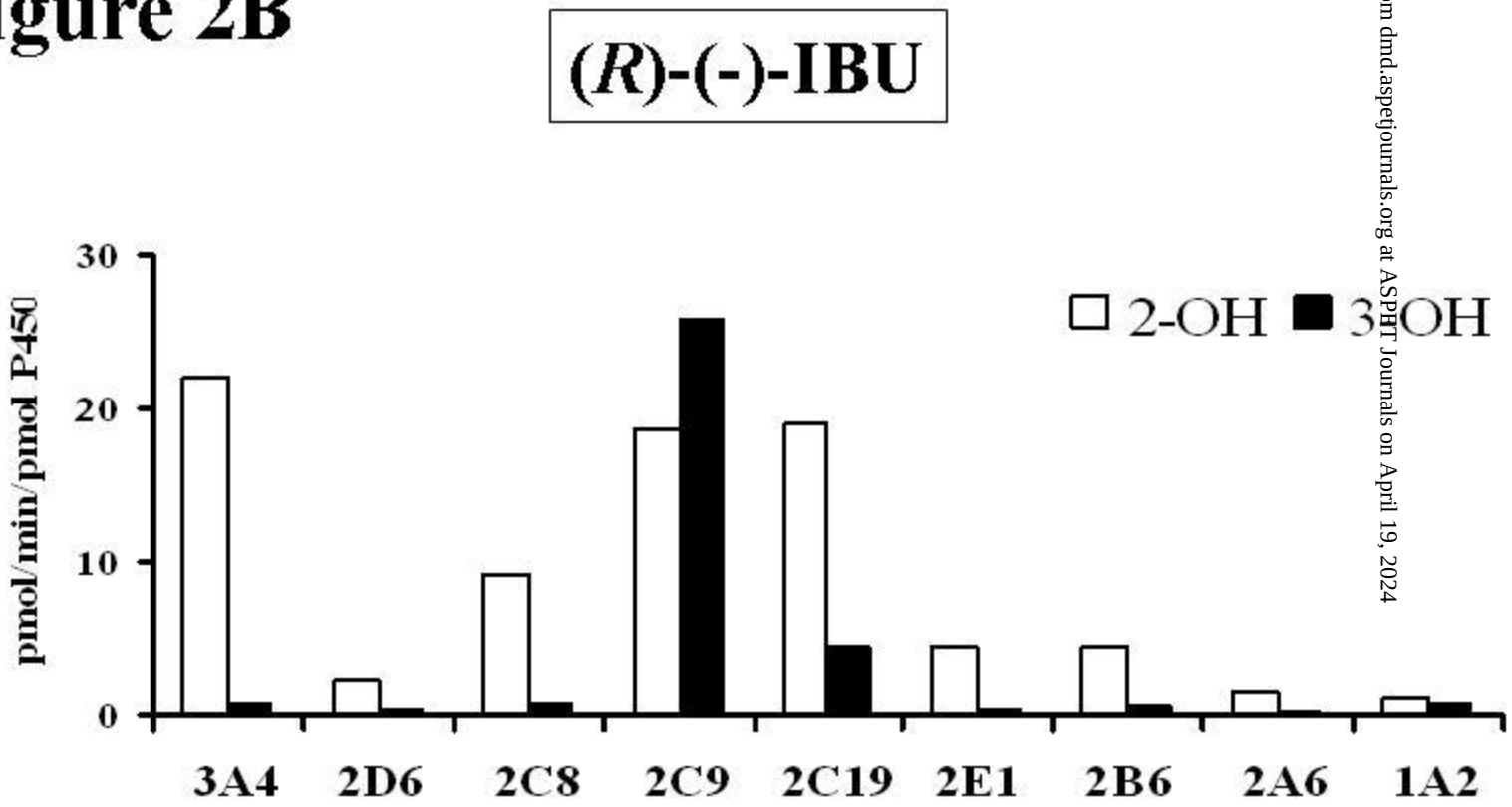

Reaction	%TNR For Each P450 Form								
	3A4	2D6	2C8	2C9	2C19	2E1	2B6	2A6	1A2
2-OH	42	<1	11	32	6	4	3	1	<1
3-OH	3	<1	2	89	3	<1	<1	<1	<1

Figure 3A

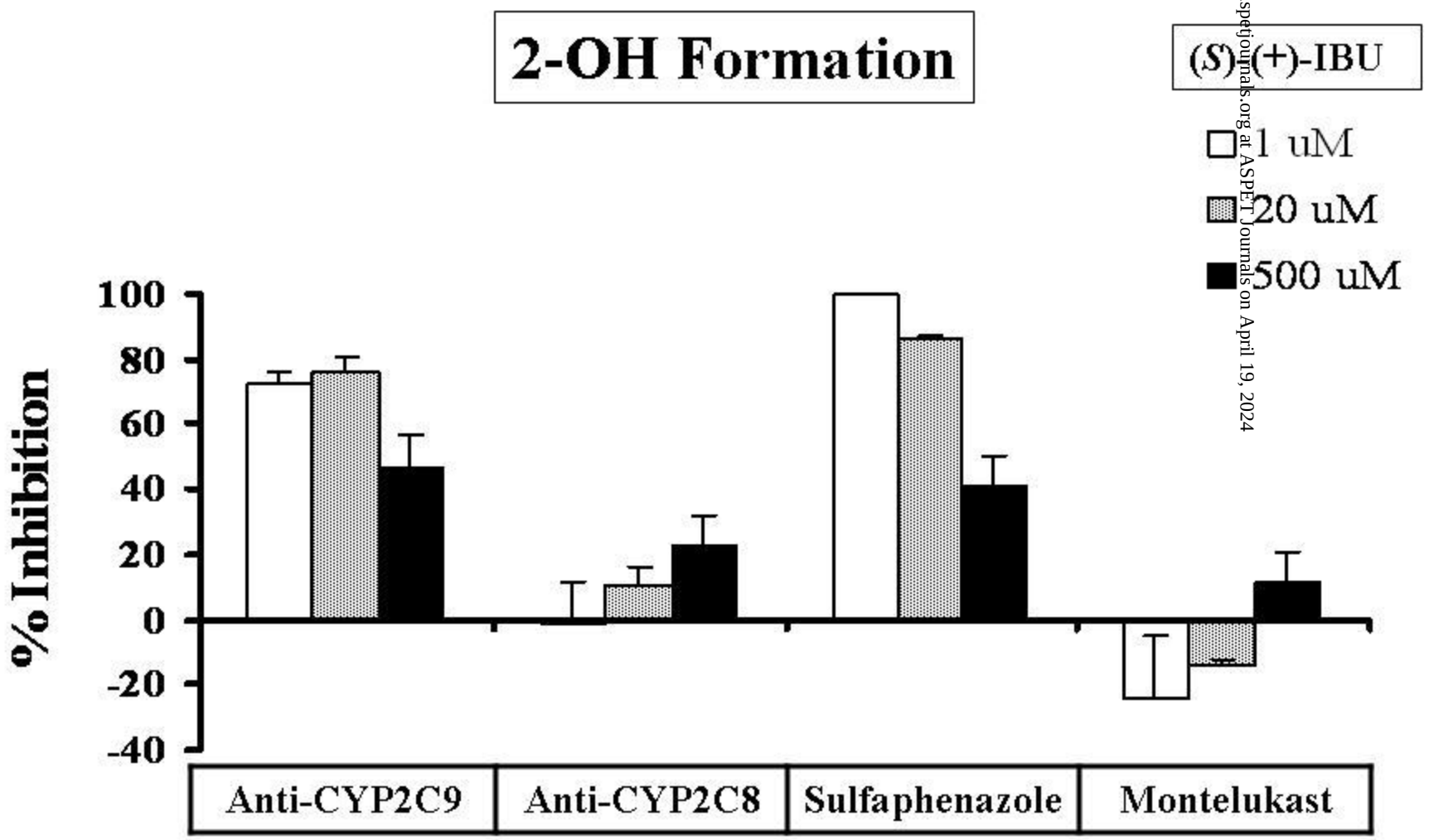

Figure 3B

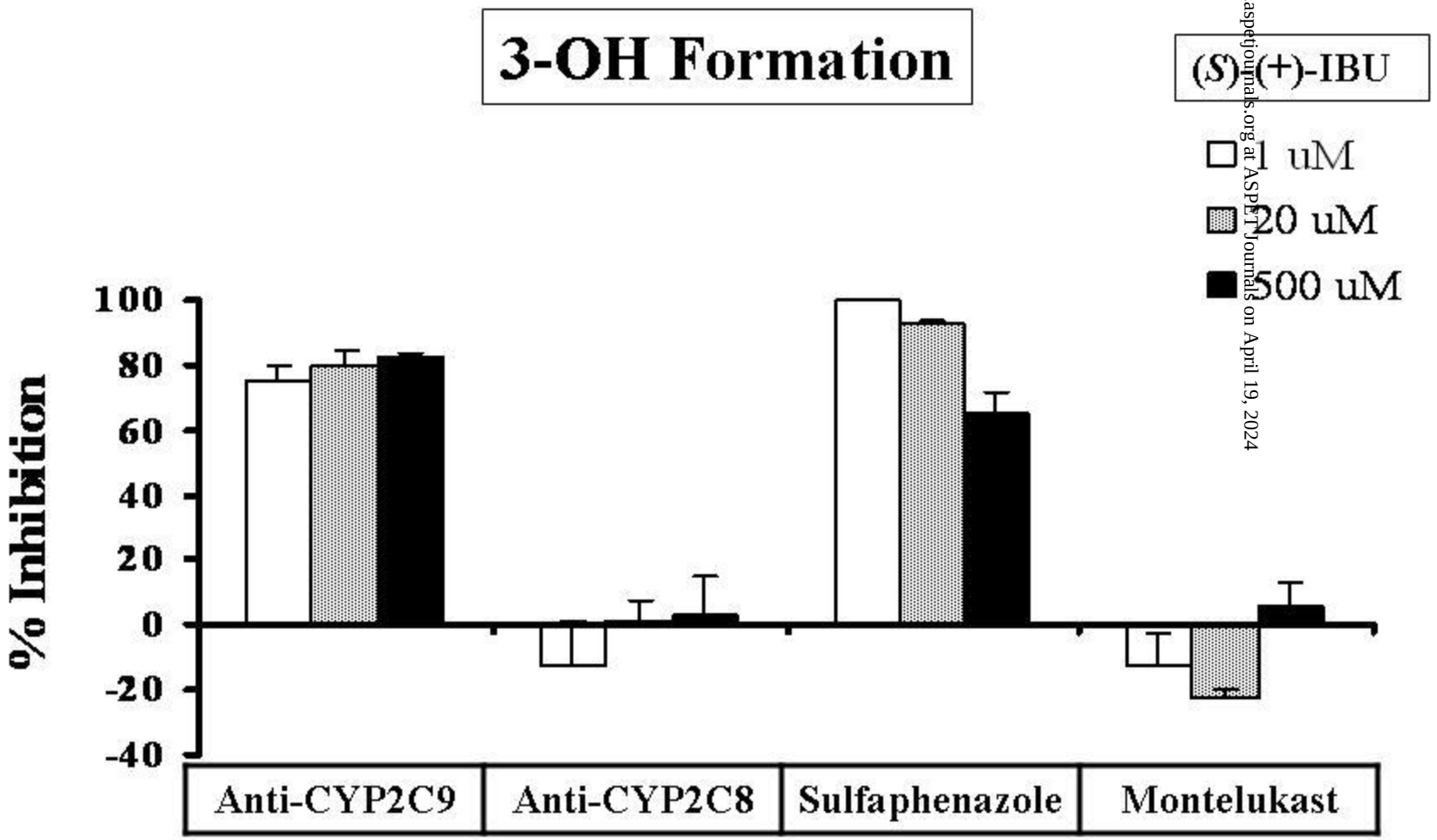

Figure 4A

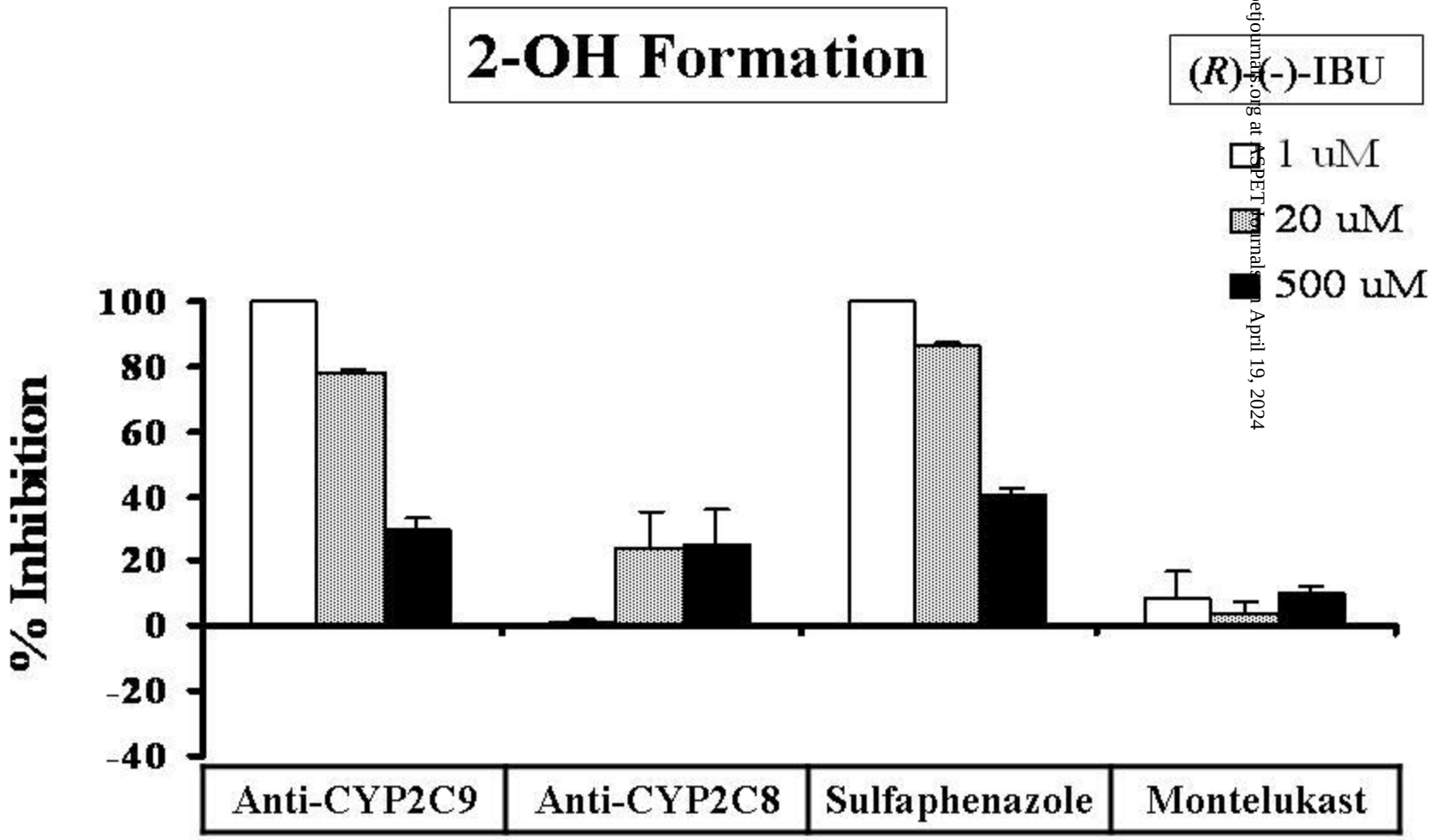

Figure 4B

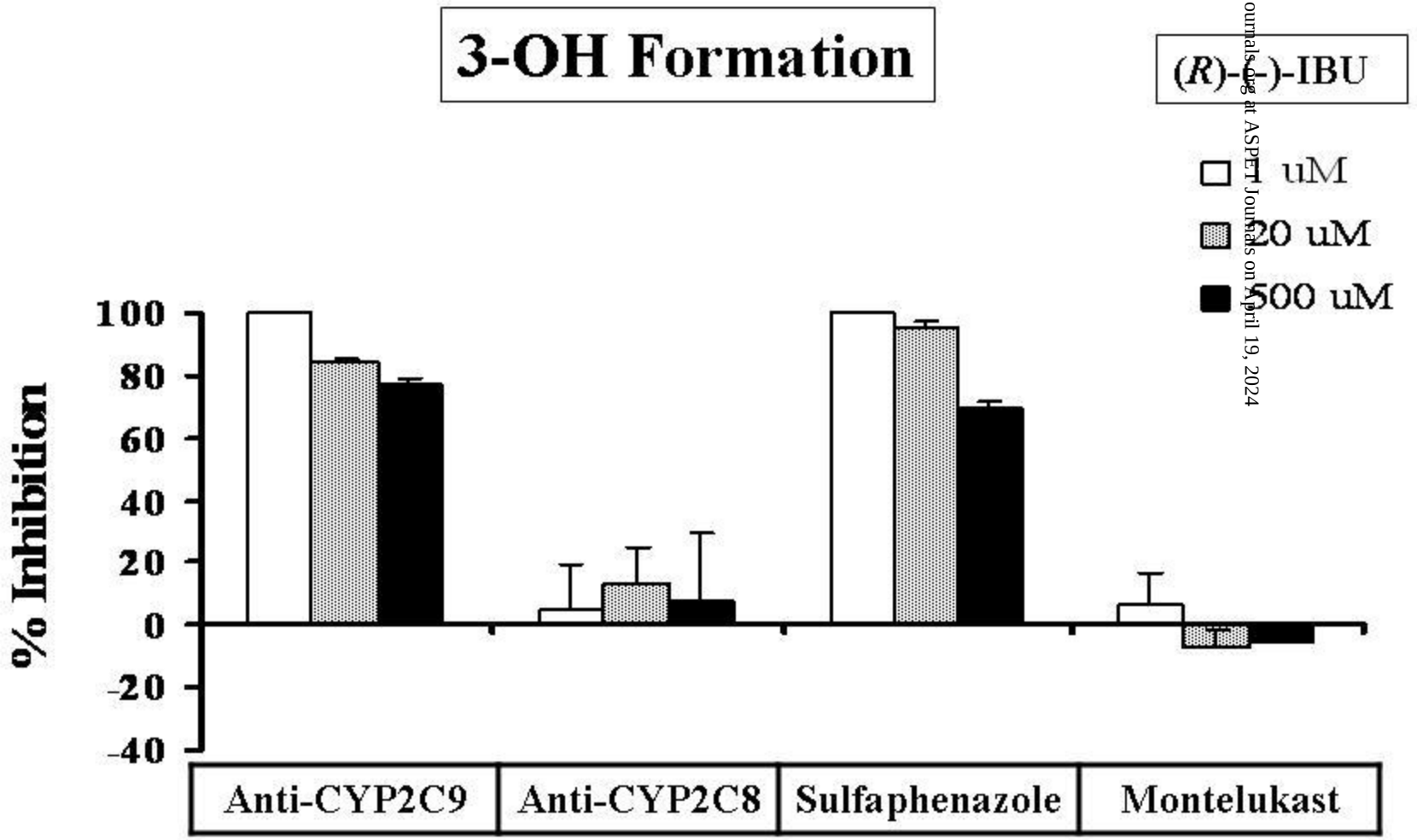

Figure 5A

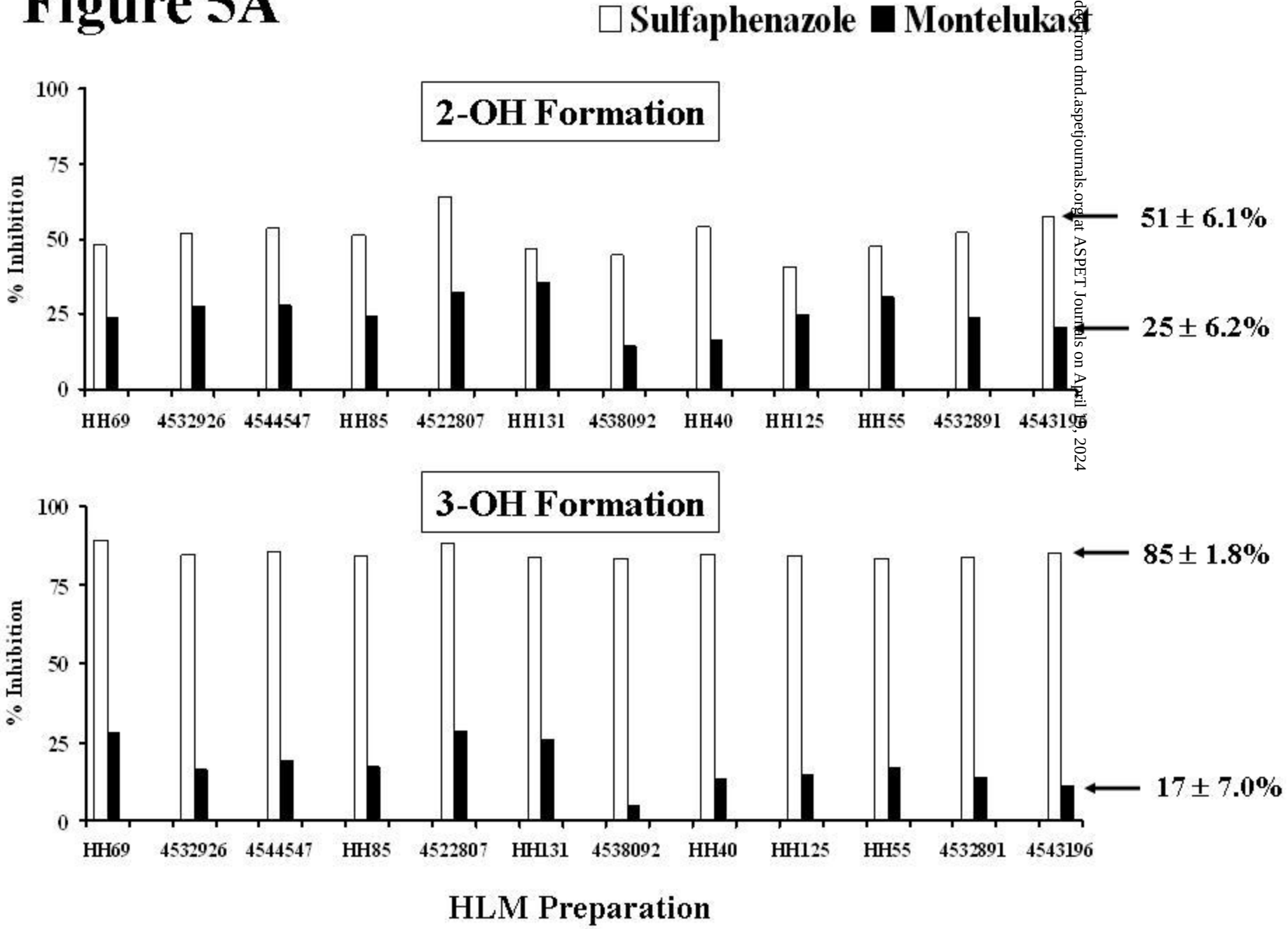

Figure 5B